Ritter's dam break model: when and where did a water column begin to move?

Eric Deleersnijder, 20 March 2025 - 25 December 2025

Contents

Abstract 1
Motivation 1
The Ritter model 3
Age: definition and constraints established *a priori* 5
Calculating the water age 7
Water age based diagnoses 8
A posteriori verification and interpretation 9
Water age distribution function 10
Illustration 12
Conclusion 13
Acknowledgements 15
References 15

Abstract. We revisit Ritter's highly idealised dam break flow model, with the aim of developing presumably novel diagnoses thereof. We use some of CART's (Constituent-oriented Age and Residence time Theory, http://www.climate.be/cart) tools in order to evaluate every water column age, i.e., the time elapsed it started moving. In the process, we also derive two types of water age distribution functions as well as the starting time and location of every water column. For all of the aforementioned diagnoses, we obtain self-similar, analytical expressions. An approach independent of CART is also adopted, which leads to similar solutions, thereby yielding some form of cross-validation. We provide a concrete illustration of the obtained results by loosely seeking inspiration in the issues faced by Zambezi River's Kariba dam.

Motivation

The failure of dams (Figure 1) and other hydraulic structures has been a matter of concern for centuries (e.g., McCullough 1968, Soares-Frazao 2002, Duffaut 2013, Perera et al. 2021, Moreno-Rodenas 2025)[1]. In this context, Ritter (1892) developed a highly idealised, frictionless, free-surface dam break flow model based on the time-dependent, one-dimensional Saint-Venant equations. Ritter derived their exact, analytical solution, which is self-similar and may be comprehended through the theory of characteristics (e.g., Sturm 2001).

[1] See also the footage of the failure of a tailings dam that took place on 25 January 2019 near Brumadinho (Brazil): https://youtu.be/sKZUZQytads?si=jqHEEjTF7JPgB2vm (last viewed on 16 March 2025)

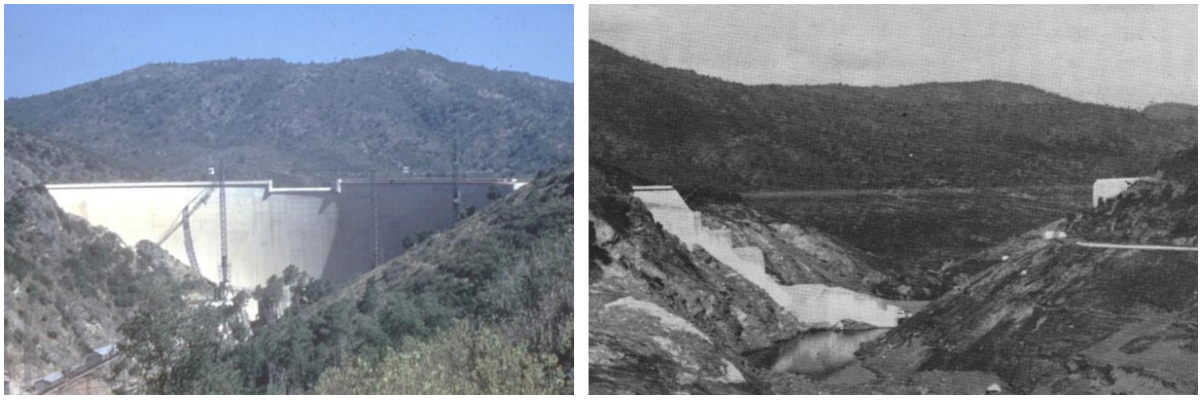


Figure 1. Left panel: Malpasset arch dam (southern France) at the end of its construction (summer 1954). Right panel: the remains of the dam, which suddenly collapsed on 2 December 1959, killing 400 to 500 human beings and wreaking havoc down to the city of Fréjus. Source: Duffaut (2013).

Nowadays Ritter's approach is still in use. It provides a benchmark for assessing numerical models and prompts new developments (e.g., Soares-Frazao 2002, Dewals et al. 2016, Castro-Orgaz and Chanson 2017, Deleersnjder 2018).

In Ritter's model, the dam reservoir is semi-infinite, flat-bottomed and initially motionless. The dam is assumed to vanish (i.e., it completely collapses) instantly. Then, a gravity wave propagates into the reservoir in the upstream direction, progressively setting water in motion. It may be instructive to calculate when and where a water parcel started moving. To the best of my knowledge, no study ever tackled this problem in a comprehensive manner. Hereinafter, we will do so by means of some of the tools of CART (Constituent-oriented Age and Residence time Theory)[2].

Below the time elapsed since a water parcel began moving is termed “age”. The latter will be calculated by solving CART's partial differential equation governing the aforementioned timescale. It must be stressed, however, that this will not be a straightforward application of CART. First, the boundaries of the domain of interest are moving, whereas most CART application have dealt with fixed boundaries, with the exception of the sea surface — whose displacement posed neither conceptual nor computational problem. What is more, the absence of diffusive processes causes the water age equation (which is originally of a parabolic nature as may be seen in, for instance Delhez et al. 1999) to simplify to a first-order hyperbolic one, so that imposing an arbitrary boundary condition at both the upstream boundary and the downstream one is theoretically impossible (whereas there would be no insuperable difficulty if the equation at hand were a parabolic one). In other words, for the obtained age to be credible, the upstream and downstream boundary conditions must be related by a physically- and mathematically-grounded consistency condition. Finally, there is no comprehensive validation of the obtained age field. This is because water parcels are not equipped with clocks! However, relevant quantitative pieces of information may be derived without using CART's equation, thereby providing independent elements of validation.

[2] See http://www.climate.be/cart and references therein (last viewed on 17 March 2025)

The Ritter model

Let t and x denote the time and the horizontal coordinate orthogonal to the dam, respectively. These independent variables obey inequalities

$$0 < t < \infty \ , \quad -\infty < x < \infty \tag{1}$$

The dam is located at $x = 0$ and the reservoir is defined by $-\infty < x \leq 0$. The dam suddenly collapses at $t = 0$. The bottom of the domain is flat and horizontal, whilst the upper boundary (i.e., the water-air interface) is free.

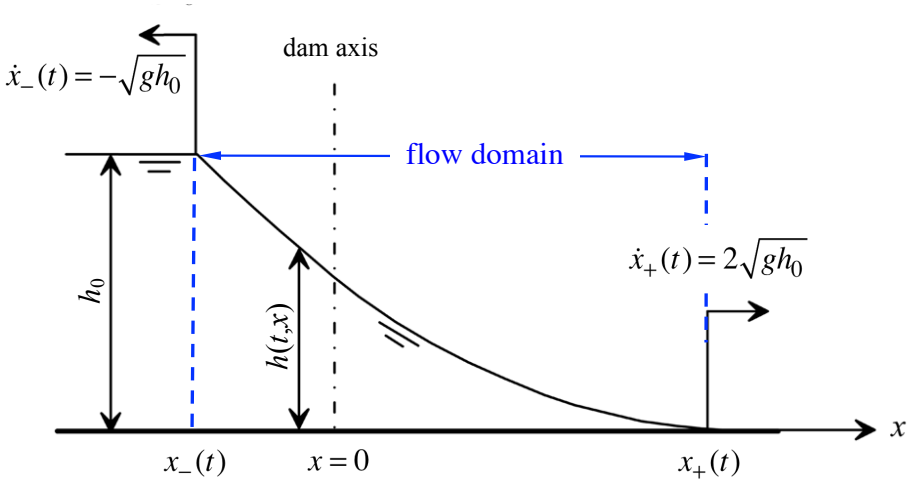


Figure 2. Free surface (water-air interface) at time t. The dam collapsed at time $t = 0$. The velocities of the upstream and downstream flow domain boundaries are denoted $\dot{x}_-$ and $\dot{x}_+$, repectively. This figure is adapted from Figure 2 of Castro-Orgaz and Chanson (2017).

In the abovementioned domain, non dissipative, one-dimensional, Saint-Venant equations are to be tackled. The continuity equation reads

$$\frac{\partial h}{\partial t} + \frac{\partial}{\partial x}(hu) = 0 \tag{2}$$

where $h(t,x)$ denotes the water height, whilst $u(t,x)$ is the water velocity, which is assumed to be independent of the vertical coordinate. The horizontal momentum equation is

$$\frac{\partial (hu)}{\partial u} + \frac{\partial}{\partial x}\left(hu^2 + \frac{gh^2}{2} \right) = 0 \tag{3}$$

where constant g is the gravitational acceleration. Partial differential equations (2)-(3) are to be solved under initial conditions

$$u(0,x) = 0 \ , \quad h(0,x) = \begin{cases} 0 \ , & 0 < x \\ h_0 \ , & x < 0 \end{cases} \tag{4}$$

The solution to partial differential problem (1)-(4) is (e.g., Ritter 1892)

$$h(t,x) = \begin{cases} 0\ ,\ x_+(t) < x \\ \dfrac{1}{9g}\left[2\sqrt{gh_0} - x/t\right]^2\ ,\ x_-(t) \le x \le x_+(t) \\ h_0\ ,\ x < x_-(t) \end{cases} \tag{5}$$

and

$$u(t,x) = \begin{cases} 0\ ,\ x_+(t) < x \\ \dfrac{2}{3}\left[\sqrt{gh_0} + x/t\right],\ x_-(t) \le x \le x_+(t) \\ 0\ ,\ x < x_-(t) \end{cases} \tag{6}$$

where $x_-(t) = -t\sqrt{gh_0}$ and $x_+(t) = 2t\sqrt{gh_0}$ refer to the upstream boundary and the downstream one of the flow domain, i.e., the domain in which the flow induced by the dam failure actually takes place (Figure 2). In other words, the flow domain is defined by inequalities $x_-(t) \le x \le x_+(t)$.

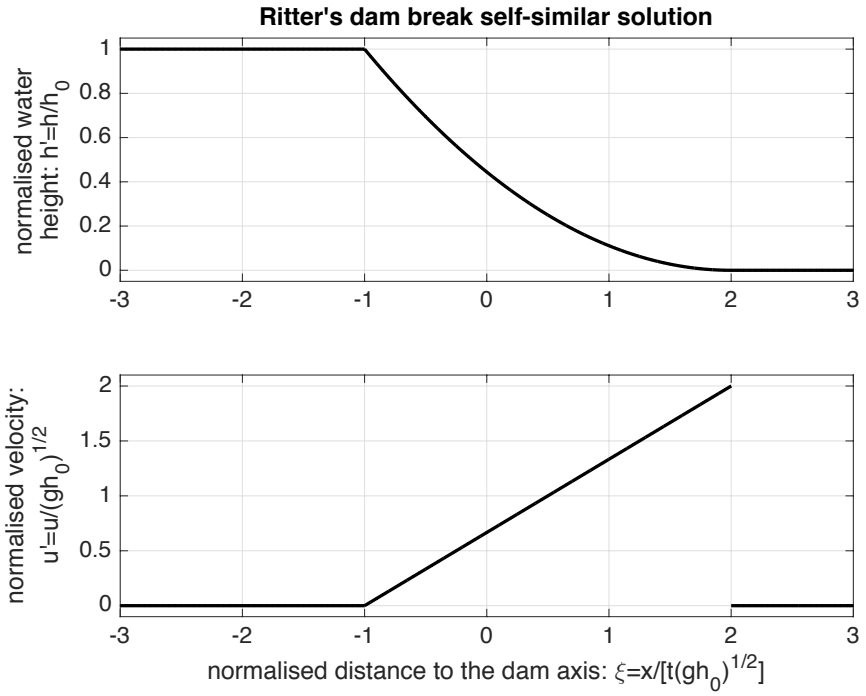


Figure 3. Representation of the water height and water velocity following Ritter's solution. The latter is self-similar: the aforementioned variables are functions of dimensionless variable $\xi = x/\left(t\sqrt{gh_0}\right)$ alone. See also Lambrechts (2025).

Ritter's solution is self-similar: it may be expressed in terms of only one variable, namely normalised (and dimensionless) distance to the dam axis

$$\xi = \frac{x/t}{\sqrt{gh_0}} = \frac{3x}{x_+(t) - x_-(t)} \tag{7}$$

with

$$-1 \leq \xi \leq 2 \tag{8}$$

Then, in the flow domain $(-1 \leq \xi \leq 2)$, the water height and the velocity may be rewritten as follows:

$$h(\xi) = \frac{h_0}{9}(2-\xi)^2 \tag{9}$$

$$u(\xi) = \frac{2\sqrt{gh_0}}{3}(1+\xi) \tag{10}$$

Accordingly, Figure 3, which is based on (9)-(10), contains all of the relevant information about Ritter's solution. The volume (per unit length in the direction parallel to the dam) of water present in the flow domain is

$$V(t) = \underbrace{-\dot{x}_-}_{=\sqrt{gh_0}} h_0 t = \int_{x_-(t)}^{x_+(t)} h(t,x)\,dx = \sqrt{gh_0^3}\,t \tag{11}$$

Age: definition and constraints established *a priori*

Herein the age of a water parcel is defined as the time elapsed since it began moving. To fully grasp this definition, a few explanatory words about the concept of "water parcel" are needed.

CART's water age partial differential problem takes into account (turbulent) diffusive processes (e.g., Delhez et al. 1999). However, in the present case, these phenomena are neglected. Therefore, the water age actually is that of a water parcel, i.e., en elemental volume whose velocity is that of the water (e.g., Lucas and Deleersnijder 2020). As the horizontal velocity does not depend on the vertical coordinate, the age of a water parcel is equivalent to the age of the water column in which this water parcel is located.

Water age $a(t,x)$ is defined in the space-time domain in which water is flowing, i.e., $0 \leq t$ and $x_-(t) \leq x \leq x_+(t)$. The velocity of the upstream boundary is

$$\dot{x}_- \triangleq \frac{d}{dt}x_-(t) = -\sqrt{gh_0} \tag{12}$$

and that of the downstream boundary reads

$$\dot{x}_+ \triangleq \frac{d}{dt}x_+(t) = 2\sqrt{gh_0} \tag{13}$$

Obviously, the age must satisfy the following boundary conditions

$$a[t,x_-(t)] = 0 \tag{14}$$

$$a[t,x_+(t)] = t \tag{15}$$

and inequalities

$$0 \leq a(t,x) \leq t \tag{16}$$

Since the upstream boundary moves at a constant speed, the flux of zero age water parcels crossing this boundary is constant. Therefore, in the vicinity of the upstream boundary, the age must obey asymptotic relation

$$a(t,x) \sim \frac{[x - x_-(t)]}{\sqrt{g h_0}} \quad , \quad x - x_-(t) \to 0^+ \tag{17}$$

A global diagnosis may also be worth examining. Let τ be the age considered as an independent variable (e.g., Delhez et al. 1999, Dewals et al. 2020). At time t, the fraction of the flow domain in which the water age lies in the interval $[\tau, \tau + \delta\tau]$ tends to $\mu(t,\tau)\delta\tau$ in the limit $\delta\tau \to 0$, where $\mu(t,\tau)$ is termed the "flow domain averaged age water age distribution function" (e.g., Dewals et al. 2024). Obviously, the physical dimension of this distribution function is time^{-1}. Since water parcels enter the flow domain through the upstream boundary, where their age is prescribed to be zero, and do not leave it later on, we easily obtain

$$\mu(t,\tau) = \frac{\left|\dot{x}_-(t-\tau)\right| \Upsilon(t-\tau)}{\int_0^t \left|\dot{x}_-(t-\tau)\right| d\tau} \tag{18a}$$

where Υ is the Heaviside function, i.e., $\Upsilon(t-\tau)$ is equal to unity if $t > \tau$ and is equal to zero otherwise. As velocity $\dot{x}_-$ is time-independent, (18a) simplifies to

$$\mu(t,\tau) = \frac{\Upsilon(t-\tau)}{t} \tag{18b}$$

meaning that the water age is homogeneously distributed in the flow domain (Figure 4). As it must, the abovementioned distribution function satisfies

$$\int_0^\infty \mu(\tau)\, d\tau = \frac{1}{t}\int_0^\infty \Upsilon(t-\tau)\, d\tau = \frac{1}{t}\underbrace{\int_0^t d\tau}_{=t} = 1 \tag{19}$$

Therefore, the flow domain averaged water age (e.g., Dewals et al. 2024) reads

$$\overline{a}(t) = \int_0^\infty \mu(\tau)\,\tau\, d\tau = \frac{1}{t}\underbrace{\int_0^t \tau\, d\tau}_{=t^2/2} = \frac{t}{2} \tag{20}$$

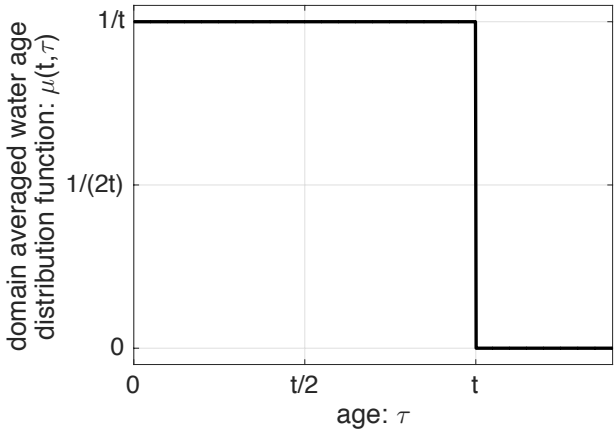


Figure 4. Flow domain averaged water age distribution function following relation (18b), i.e., $\mu(t,\tau) = \Upsilon(t-\tau)/t$.

Calculating the water age

In accordance with Delhez et al. (1999), the water is treated as a passive or inert tracer (i.e., a tracer that undergoes no reaction) whose concentration is equal to unity at any time and position. Therefore, the age concentration equation is equivalent to the age equation. In the framework of a depth-integrated approach (e.g. de Brye et al. 2012, Pham Van et al. 2020) and in the absence of diffusive processes, the water age is governed by partial differential equation

$$\frac{\partial}{\partial t}(ha) + \frac{\partial}{\partial x}(hua) = h \tag{21}$$

Combining this equation with continuity equation (2) yields

$$D_t a = \frac{\partial a}{\partial t} + u\frac{\partial a}{\partial x} = 1 \tag{22}$$

where $D_t = \partial/\partial t + u\,\partial/\partial x$ is the material derivative operator. Unsurprisingly, (22) means that the age of a water parcel (or column) increases as the same pace as time progresses.

As Ritter's water height and velocity are self similar, it seems quite natural to assume that the solution to (22) is self similar too. Accordingly, new independent variables are to be introduced, i.e., $\theta = t$ and $\xi = x/(t\sqrt{gh_0})$. The latter variable was defined above. Therefore, the time and space derivatives transform as follows

$$\frac{\partial}{\partial t} = \underbrace{\frac{\partial \theta}{\partial t}}_{=1}\frac{\partial}{\partial \theta} + \underbrace{\frac{\partial \xi}{\partial t}}_{=-\frac{x/t^2}{\sqrt{gh_0}}}\frac{\partial}{\partial \xi} = \frac{\partial}{\partial \theta} - \frac{\xi}{\theta}\frac{\partial}{\partial \xi} \tag{23}$$

$$\frac{\partial}{\partial x} = \underbrace{\frac{\partial \theta}{\partial x}}_{=0}\frac{\partial}{\partial \theta} + \underbrace{\frac{\partial \xi}{\partial x}}_{=\frac{1/t}{\sqrt{gh_0}}}\frac{\partial}{\partial \xi} = \frac{1/\theta}{\sqrt{gh_0}}\frac{\partial}{\partial \xi} \tag{24}$$

Substituting (23)-(24) into (22) and assuming that the age is of the form $a = b(\xi)\theta$ yields (after some manipulations)

$$\frac{2-\xi}{3}\frac{db}{d\xi} + b = 1 \tag{25}$$

Dimensionless age profile $b(\xi)$ must satisfy boundary conditions

$$\underbrace{\left[b(\xi)\right]_{\xi=-1} = 0}_{\text{upstream b. c.}} \quad , \quad \underbrace{\left[b(\xi)\right]_{\xi=2} = 1}_{\text{downstream b. c.}} \tag{26}$$

eventually leading to

$$b(\xi) = 1 - \frac{(2-\xi)^3}{27} \tag{27}$$

Therefore, the water age reads (Figure 5)

$$a(\theta,\xi) = \left[1 - \frac{(2-\xi)^3}{27}\right]\theta \quad , \quad -1 \le \xi = \frac{x/t}{\sqrt{gh_0}} \le 2 \tag{28}$$

or, equivalently,

$$a(t,x) = \frac{19t}{27} + \frac{4x}{9(gh_0)^{1/2}} - \frac{2x^2}{9gh_0t} + \frac{x^3}{27(gh_0)^{3/2}t^2} \quad , \quad \underbrace{-t\sqrt{gh_0}}_{=x_-(t)} \le x \le \underbrace{2t\sqrt{gh_0}}_{=x_+(t)} \tag{29}$$

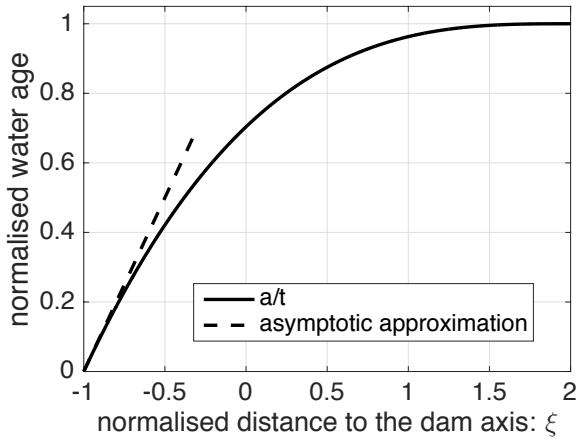


Figure 5. Normalised water age $a(t,x)/t = 1-(2-\xi)^3/27$ (solid curve) as a function of normalised distance to the dam axis $\xi = x/(t\sqrt{gh_0})$. The dashed line is associated with asymptotic approximation (30), i.e., $a(t,x)/t \sim 1+\xi$, $1+\xi \to 0^+$. The graph covers the whole flow domain ($\xi \in [-1,2]$).

Water age based diagnoses

In light of boundary conditions (26), age (28) obviously satisfies boundary conditions (14)-(15). If $\xi \in [-1,2]$, inequalities $0 \le b(\xi) \le 1$ are easily seen to hold valid, implying that age (28) satisfies (16), i.e., the water age is non negative and smaller than or equal to elapsed time t. In the vicinity of upstream boundary, (28) admits asymptotic expression

$$a(\theta,\xi) \sim (1+\xi)\theta \quad , \quad (1+\xi) \to 0^+ \tag{30}$$

which is equivalent to (17). The flow domain averaged age is

$$\overline{a}(t) = \frac{1}{V(t)} \int_{x_-(t)}^{x_+(t)} h(t,x)\, a(t,x)\, dx = \frac{t}{2} \tag{31}$$

which is equivalent to (20). Thus, all of the age properties established *a priori* are satisfied by age (28), with the exception of (18b). The latter will be derived from the age distribution function in the next Section.

In accordance with the very definition of the water age employed herein, the water column that is at time t and coordinate x began to move at (starting) time (Figure 6)

$$t_s(t,x) = t - a(t,x) \tag{32}$$

where $0 \le t_s(t,x) \le t$. By the same token, the abovementioned water column was set in motion at (starting) coordinate

$$x_s(t,x) = -\sqrt{gh_0}\,[t - a(t,x)] \tag{33}$$

where $x_(t) \le x_s(t) \le 0$, as expected. This formula is depicted in Figure 7 under the following self-similar formulation

$$\xi_s(\xi) = \frac{x_s(t,x)}{\sqrt{gh_0}\, t} = -\frac{(2-\xi)^3}{27} \tag{34}$$

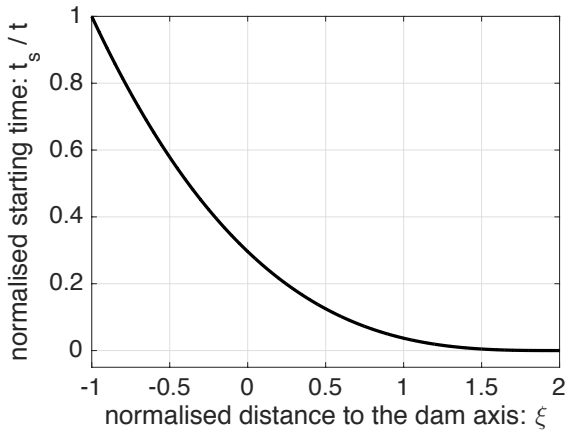


Figure 6. Normalised starting time $t_s(t,x)/t = (2-\xi)^3/27$ as a function of normalised distance to the dam axis $\xi = x/(t\sqrt{gh_0})$. The graph covers the whole flow domain $(\xi \in [-1,2])$.

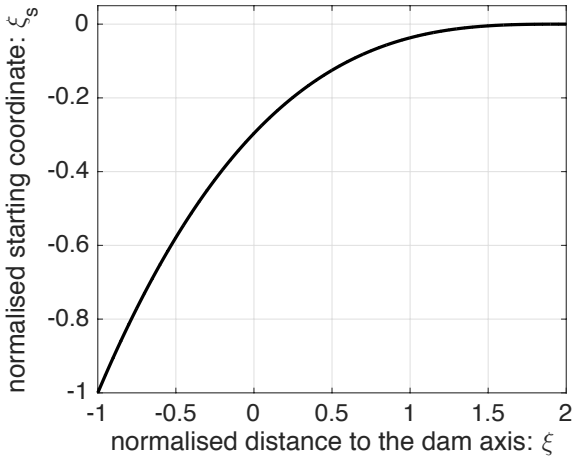


Figure 7. Normalised starting coordinate $\xi_s(\xi) = -(2-\xi)^3/27$ as a function of normalised distance to the dam axis $\xi = x/(t\sqrt{gh_0})$ following formula (34). The graph covers the whole flow domain $(\xi \in [-1,2])$.

A posteriori verification and interpretation

All of the developments carried out above helped us gain insight into the Ritter's idealised

dam break flow model. In particular, it made us realise that the water age as well as the starting time and coordinate could have been obtained without explicitly resorting to CART's tools. In this regard, the key ingredients are twofold. Firstly, diffusive processes are assumed to be negligible and, secondly, the phase speed of the gravity wave propagating into the reservoir (in the upstream direction) is constant.

At time t, the volume (per unit length in the direction parallel to the dam) of the water that is present in the flow domain downstream of coordinate x is

$$V_d(t,x) = \int_x^{x_+(t)} h(t,x)\,dx \tag{35}$$

or, equivalently,

$$V_d(\theta,\xi) = \theta\sqrt{gh_0^3}\int_\xi^2 \frac{(2-\xi')^2}{9}\,d\xi' = \frac{\sqrt{gh_0^3}}{27}(2-\xi)^3\,\theta \tag{36}$$

Then, the age of the water column located at time t at coordinate x or, equivalently, at time θ and coordinate ξ reads

$$a(\theta,\xi) = \left[1-\frac{V_d(\theta,\xi)}{V(\theta)}\right]\theta = \left[1-\frac{(2-\xi)^3}{27}\right]\theta \tag{37}$$

This expression is similar to (28). Following the same line of reasoning, the starting time and coordinate can also be derived:

$$\theta_s(\theta,\xi) = \frac{V_d(\theta,\xi)}{V(\theta)}\theta = \frac{(2-\xi)^3}{27}\theta \tag{38}$$

$$\xi_s(\theta,\xi) = -\frac{V_d(\theta,\xi)}{V(\theta)} = -\frac{(2-\xi)^3}{27} \tag{39}$$

It is readily seen that (38)-(39) are equivalent to (32)-(33).

Over a relatively long distance, the age remains close to its maximum value (t), which is located at the downstream boundary. Figure 5 clearly illustrates this striking feature. The interpretation thereof is rather elementary: as time progresses, the height of a water column decreases, implying that its width must increase in such a way that its volume remains unchanged. However, the age difference between the maximum and the minimum of the age within this water column (δa) is time-independent. This may also be investigated in a more quantitative manner. Consider a water column that at time $t=0$ is adjacent to the dam. Its initial width is denoted δx_0, implying that its volume is $\delta x_0\, h_0$, whilst the age difference is $\delta a = \delta x_0/\sqrt{gh_0}$. Later on, this water column remains adjacent to the flow domain front. Using (36), it is readily seen that its width increases as time progresses following formula $\delta x(t) = \left(27 gh_0 \delta x_0 t^2\right)^{1/3}$. This relation is valid provided $t > \delta x_0/\sqrt{gh_0}$. Needless to say, ratio $\delta a/\delta x(t)$ decreases as time goes by.

Water age distribution function

The core variable of CART's age theory is the age distribution function (e.g., Delhez et al.

1999). In the present context, the water age distribution function is denoted $c(t,x,\tau)$ and is defined as follows: at time t and coordinate x, the water volume (per unit length in the direction parallel to the dam) of the water whose age lies in the interval $[\tau,\tau+\delta\tau]$ tends to $h(t,x)c(t,x,\tau)\delta x\delta\tau$ in the limit $\delta x,\delta\tau\to 0$. Obviously, the physical dimension of this distribution function is time^{-1}.

The water age distribution function is governed by partial differential equation (e.g. Delhez and Deleersnijder 2002, Dewals et al. 2020)

$$\frac{\partial c}{\partial t} + u\frac{\partial c}{\partial x} = -\frac{\partial c}{\partial \tau} \tag{40}$$

which is to be solved under auxiliary conditions (e.g. Deleersnijder et al. 2020)

$$\left[c(t,x,\tau)\right]_{t=0} = 0 \quad , \quad \left[c(t,x,\tau)\right]_{x=x_-(t)} = \delta(\tau-0) \quad , \quad \left[c(t,x,\tau)\right]_{\tau=0} = 0 \tag{41}$$

where δ denotes the Dirac delta function. In the sense of Schwartz's distributions, the solution to partial differential problem (35)-(36) is

$$c(t,x,\tau) = \delta\left[a(t,x)-\tau\right]\Upsilon(t-\tau) \tag{42}$$

where $a(t,x)$ is given by (29).

The age distribution function may be viewed as the histogram of the ages of the particles under study that are present in an elemental volume, thereby reflecting the fact that these particles ended up in the aforementioned elemental volume through different pathways. This is why they are likely to be characterised by various ages. The "width" of the distribution function reflects, among other things, the importance of diffusive or reactive processes. Herein no such phenomena are to be taken into account. As a consequence, all the water particles present in an elemental control volume have had the same history, hence the Dirac delta function in (42).

The zeroth-order moment of $c(t,x,\tau)$ represents the water concentration and, as it must, is identically equal to unity:

$$\int_0^\infty c(t,x,\tau)\,d\tau = \int_0^t \delta\left[a(t,x)-\tau\right]d\tau = 1 \tag{43}$$

Then, in accordance with the age averaging hypothesis (Deleersnijder et al. 2001), the water age reads

$$\frac{\displaystyle\int_0^\infty c(t,x,\tau)\tau\,d\tau}{\displaystyle\int_0^\infty c(t,x,\tau)\,d\tau} = \int_0^\infty c(t,x,\tau)\tau\,d\tau = \int_0^t \delta\left[a(t,x)-\tau\right]\tau\,d\tau = a(t,x) \tag{44}$$

which is identically equivalent to (29).

In accordance with Dewals et al. (2024), the flow domain averaged water age distribution function may be derived as follows:

$$\mu(t,\tau) = \frac{1}{V(t)}\int_{x_-(t)}^{x_+(t)} h(t,x)\,c(t,x,\tau)\,dx = \frac{1}{t\sqrt{gh_0^3}}\int_{x_-(t)}^{x_+(t)} h(t,x)\,\delta\left[a(t,x)-\tau\right]\Upsilon(t-\tau)\,dx \tag{45}$$

Owing to the presence of Dirac delta function $\delta\left[a(t,x)-\tau\right]$ in integral (40), the latter cannot

be evaluated in its present form. In order to circumvent this difficulty, we will take advantage of the one-to-one correspondence between the space coordinate and the water age, which implies

$$\frac{\partial a}{\partial x} = \frac{h(t,x)}{\sqrt{gh_0^3}} \tag{46}$$

This allows transforming (45) to

$$\begin{aligned} \mu(t,\tau) &= \frac{1}{t\sqrt{gh_0^3}} \int_0^t \frac{h(t,x)\, c(t,x,\tau)}{\partial a / \partial x}\, da = \frac{1}{t\sqrt{gh_0^3}} \int_0^t \frac{h(t,x)\, \delta\big[a(t,x)-\tau\big]}{h(t,x)/\sqrt{gh_0^3}}\, da \\ &= \frac{1}{t} \int_0^t \delta\big[\tau - a\big] \Upsilon(t-\tau)\, da = \frac{\Upsilon(t-\tau)}{t} \end{aligned} \tag{47}$$

As expected, (47) is equivalent to (18b).

Illustration

Most of the results derived above are self-similar expressions. Therefore, grasping the actual order of magnitude of the key diagnostic variables is not that straightforward. This is why a somewhat concrete illustration is worth considering.

There are several major dams that have been or should be rehabilitated so as to avoid major disasters (Perera et al. 2021). For instance, the gigantic Zambezi River Kariba dam (Figure 8), which is located on the border between Zambia and Zimbabwe and has the world's largest reservoir, has undergone costly repairs[3] aimed, among other things, at stopping the scouring at the floor of its plunge pool, which takes place when floodgates are open[4]. Since the dam began operations in 1959, the plunge pool has significantly expanded; its depth has increased from 10 m to about 90 m (e.g., Duarte et al. 2016). If nothing had been done, the dam would have collapsed sooner or later. Coincidentally or not, the Malpasset and Kariba arch dams were designed by the same engineering firm.

If the Kariba dam were to collapse, a disaster akin to the Biblical flood would occur. To realize that this metaphor is hardly an exaggeration, Ritter's solution might be resorted to with $h_0 \approx 120$ m. This would definitely not lead to reliable values but would, hopefully, yield instructive orders of magnitude. For instance, according to Ritter's solution, the edge of the flood wave would progress at a speed of order $2\sqrt{gh_0} \approx 250$ km/h. It would most likely reach the Indian Ocean, killing or rendering homeless countless human beings. In this instance, the tale of the sorcerer's apprentice might be worth keeping in mind...

Based on $h_0 \approx 120$ m, the water age, the starting time and the starting coordinate are depicted at $t = 5, 10, 15$ minutes in Figures 8, 9 and 10. In addition, Figure 11 represents the evolution of the water age at the locations of the dam axis $(x = 0)$, i.e., $a(t, x = 0) = (19/27)t$.

[3] https://projects.worldbank.org/en/projects-operations/project-detail/P146515 (last viewed on 18 March 2025)

[4] A footage of the operation of the Kariba dam flood gates (whose inadequate design caused the scouring process illustrated in the lower panel of Figure 8) is available at URL https://youtu.be/qDnkfO3g63s?si=HdUfXUWO5KLajlva (last viewed on 18 March 2025)

Clearly, this age increases at a pace slower than that at which time progresses. The orders of magnitude of the variables illustrated in these figures are mind boggling. Nonetheless, it must be recalled that they should not be taken at face value.

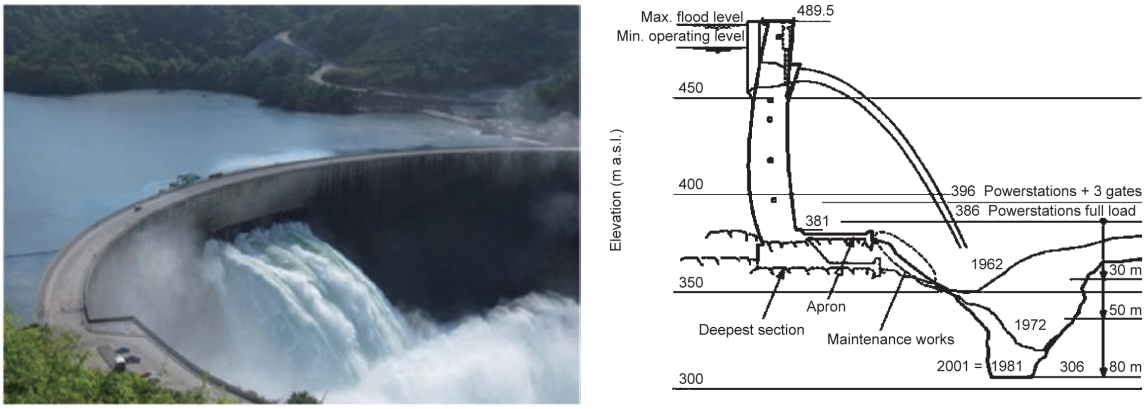


Figure 8. Left panel: aerial photograph of the Zambezi River Kariba dam, which is located on the border between Zambia and Zimbabwe and has the world's largest reservoir (Figure 6 of Duarte et al. 2016). Right panel: illustration of the time evolution of the plunge pool scour hole (Figure 7 of Duarte et al. 2016).

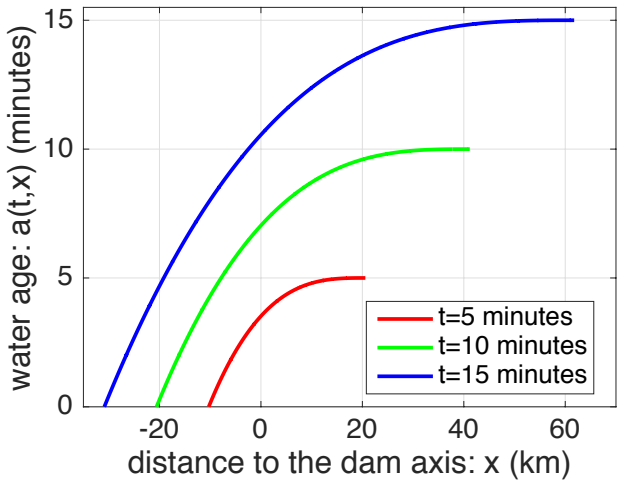


Figure 9. Representation at different instants ($t = 5, 10, 15$ minutes) of water age $a(t,x)$ as a function of the distance to the dam axis (x) assuming that $g = 9.81\ \text{m/s}^2$ and $h_0 = 120$ m . See also Lambrechts (2025).

Conclusion

We have adopted various approaches to derive the same diagnostic variables. All of the obtained analytical expressions are consistent with each other, thereby providing some form

of cross-validation of them. This is perhaps the first application of CART to a non-diffusive, moving boundary problem, that, what is more, admits a comprehensive validation by means of pieces of information unrelated to CART.

Unfortunately, we have not fully unravelled the very reason why the upstream and downstream age boundary conditions can be met despite the fact that the underlying partial differential equation is a first-order hyperbolic one. This undoubtedly reveals that the partial differential problem at hand is mathematically and physically well posed.

It remains to be seen whether or not the results derived in the present working note or only the methodology resorted to above will be of use to realistic dam break or wetting-drying studies.

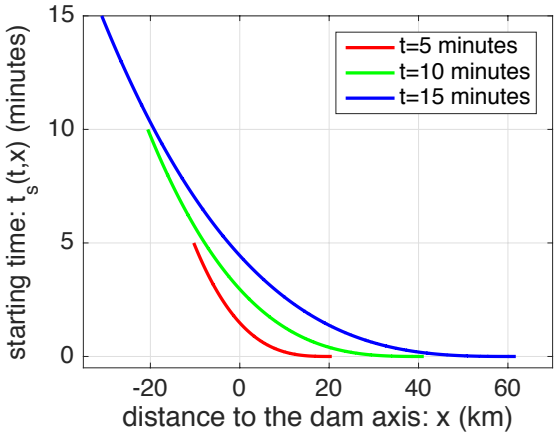


Figure 10. Representation at different instants ($t = 5, 10, 15$ minutes) of starting time $t_s(t,x) = t - a(t,x)$ as a function of the distance to the dam axis (x) assuming that $g = 9.81\ \text{m/s}^2$ and $h_0 = 120$ m .

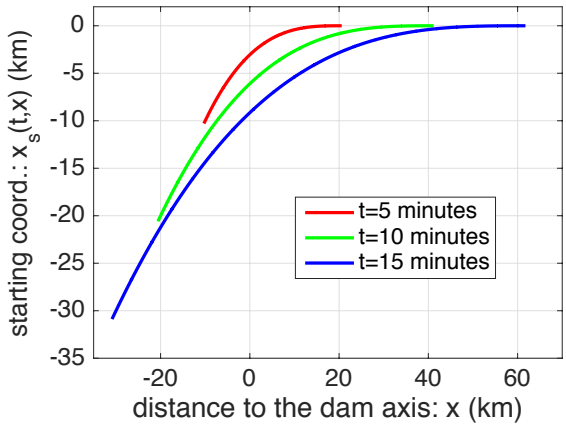


Figure 11. Representation at different instants ($t = 5, 10, 15$ minutes) of starting coordinate $x_s(t,x) = -\sqrt{gh_0}\,[t - a(t,x)]$ as a function of the distance to the dam axis (x) assuming that $g = 9.81\ \text{m/s}^2$ and $h_0 = 120$ m .

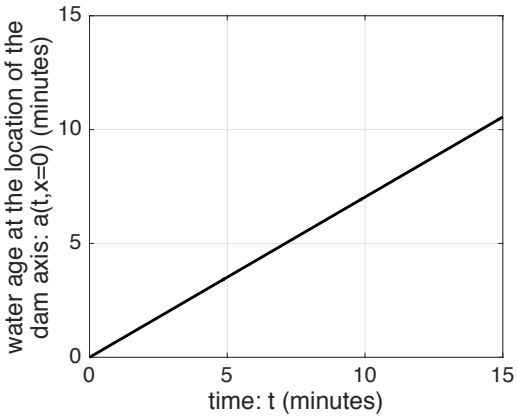


Figure 12. Time evolution of the water age at the location of the dam axis, i.e., $a(t, x = 0) = (19 / 27)t$.

Acknowledgements. Benjamin Dewals provided useful pieces of information and advice. Jonathan Lambrechts made the animation CART_Ritter.mp4.

References

Castro-Orgaz O. and H. Chanson, 2017, Ritter's dry-bed dam-break flows: positive and negative wave dynamics, *Environmental Fluid Mechanics*, 17, 665-694

de Brye B., A. de Brauwere, O. Gourgue, E.J.M. Delhez and E. Deleersnijder, 2012, Water renewal timescales in the Scheldt Estuary, *Journal of Marine Systems*, 94, 74-86

Deleersnijder E., 2018, *Establishing the consistency of the asymptotic formula of Deleersnijder (2002) with the exact one-dimensional dam break flow solution of Ritter (1892)*. Working note, Université catholique de Louvain, Louvain-la-Neuve, Belgium, 4 pages, available at URL http://hdl.handle.net/2078.1/196717

Deleersnijder E., J.-M. Campin and E.J.M. Delhez, 2001, The concept of age in marine modelling: I. Theory and preliminary model results, *Journal of Marine Systems*, 28, 229-267

Deleernijder E., I. Draoui, J. Lambrechts, V. Legat and A Mouchet, 2020, Consistent boundary conditions for age calculations, *Water*, 12, 1274, doi: 10.3390/w12051274

Delhez E.J.M., J.-M. Campin, A.C. Hirst and E. Deleersnijder, 1999, Toward a general theory of the age in ocean modelling, *Ocean Modelling*, 1, 17-27

Delhez E.J.M. and E. Deleersnijder, 2002, The concept of age in marine modelling: II. Concentration distribution function in the English Channel and the North Sea, *Journal of Marine Systems*, 31, 279-297

Dewals B., P. Archambeau, M. Bruwier, S. Erpicum, M. Pirotton, T. Adam, E.J.M. Delhez and E. Deleersnijder, 2020, Age of water particles as a diagnosis of steady-state flows in

shallow rectangular reservoirs, *Water*, 12, 2819, doi: 10.3390/w12102819

Dewals B., P. Archambeau, S. Erpicum, M. Pirotton and E. Deleersnijder, 2024, What does the volume-averaged water age distribution function reveal about flow fields in rectangular shallow reservoirs?, *Environmental Fluid Mechanics*, 24, 75-93

Dewals B., M. Bruwier, S. Erpicum, M. Pirotton and P. Archambeau, 2016, Energy conservation properties of Ritter solution for idealized dam break flow, *Journal of Hydraulic Research*, 54, 581-585

Duarte R., A. Pinheiro and A.J. Schleiss, 2016, An enhanced physically based scour model for considering jet air entrainment, *Engineering*, 2, 294-301

Duffaut P., 2013, The traps behind the failure of the Malpasset arch dam, France, in 1959, *Journal of Rock Mechanics and Geotechnical Engineering*, 5, 335-341

Lambrechts J., 2025, Animation in mp4 format, available at URL https://perso.uclouvain.be/eric.deleersnijder/CART_Ritter.mp4

Lucas L.V. and E. Deleersnijder, 2020, Timescale methods for simplifying, understanding and modeling biophysical and water quality processes in coastal aquatic ecosystems: a review, *Water*, 12, 2717, doi: 10.3390/w12102717

Moreno-Rodenas A., Mantilla-Jones J.D. and D. Valero, 2025, Age, climate and economic disparities drive the current state of global dam safety, *Nature Water*, 3, 284-295

Perera D., V. Smakhtin, S. Williams, T. North and A. Curry, 2021, *Ageing Water Storage Infrastructure: An Emerging Global Risk*, UNU-INWEH Report Series, Issue 11, United Nations University Institute for Water, Environment and Health, Hamilton, Canada, 31 pages

Pham Van C., B. de Brye, A. de Brauwere, A.J.F. Hoitink, S. Soares-Frazao and E. Deleersnijder, 2020, Numerical simulation of water renewal timescales in the Mahakam Delta, Indonesia, *Water*, 12, 1017, doi: 10.3390/w12041017

Ritter A., 1892, Die Fortpflanzung von Wasserwellen, *Zeitschrift Verein Deutscher Ingenieure*, 36(2), 947-954

Soares Frazão S., 2002, *Dam-break induced flows in complex topographies. Theoretical, numerical and experimental approaches*, Doctoral dissertation, Université catholique de Louvain, Louvain-la-Neuve, Belgium, 240 pages, available at URL https://hdl.handle.net/2078.1/206214

Sturm T., 2001, *Open Channel Hydraulics*, McGraw-Hill Series in Water Resources and Environmental Engineering, 493 pages

---